Exploring the enantiomeric 13C position-specific isotope fractionation: challenges and anisotropic NMR-based analytical strategy

Philippe Lesot, Philippe Berdagué, Virginie Silvestre, Gérald Remaud

Exploring the Enantiomeric ^{13}C Position-Specific Isotope Fractionation: Challenges and Anisotropic NMR-based Analytical Strategy

Philippe Lesot[a,b*], **Philippe Berdagué**[a], **Virginie Silvestre**[c] **and Gérald Remaud**[c,*]

[a] Université de Paris-Saclay, RMN en Milieu Orienté, ICMMO, CNRS UMR 8182, RMN en Milieu Orienté, Bât. 410, rue du Doyen Georges Poitou, F-91405 Orsay cedex, France.

[b] Centre National de la Recherche Scientifique (CNRS), 3 rue Michel Ange, F-75016 Paris, France.

[c] Université de Nantes, CNRS UMR 6230, CEISAM, F-44000, Nantes France.

ABSTRACT:

Trying to answer the intriguing and fundamental question related to chiral induction/amplification at the origin of homochirality in Nature: "Is there a relationship between enantiomeric and isotopic fractionation of carbon 13 in chiral molecules?" is a difficult but stimulating challenge. Although isotropic ^{13}C-PSIA NMR is a promising tool for determination of ($^{13}C/^{12}C$) ratios capable of providing key ^{13}C isotopic data for understanding the reaction mechanisms of biological processes or artificial transformations, this method does not provide access to any enantiomeric ^{13}C isotopic data unless mirror-image isomers are first physically separated. Interestingly, ^{13}C spectral enantiodiscriminations can be potentially performed *in situ* in presence of enantiopure entities as chiral-europium complexes or chiral liquid crystals (CLCs). In this work, we explored for the first time the capabilities of the anisotropic ^{13}C-{^{1}H} NMR using PBLG-based lyotropic CLCs as enantiodiscriminating media in the context of the enantiomeric position-specific ^{13}C isotope fractionation (EPSIF), within the requested precision of the order of the permil. As enantiomeric NMR signals are discriminated on the basis of a difference of ^{13}C residual chemical shift anisotropy (^{13}C-RCSA) prior to be deconvoluted, analysis of enantiomeric mixtures becomes possible. The analytical potential of this approach when using poly-□-benzyl-*L*-glutamate (PBLG) is presented, and the preliminary quantitative results on small model chiral molecules obtained at 17.5 T with a cryogenic NMR probe are reported and discussed.

Keywords ^{13}C-{^{1}H} NMR . ^{13}C-RCSA, ($^{13}C/^{12}C$) ratio . Enantiomeric isotopic fractionation . Polypeptide liquid crystals . Chirality

Corresponding authors: philippe.lesot@universite-paris-saclay.fr

gerald.remaud@univ-nantes.fr

Supporting information: Supporting information available

ORCID numbers : - Philippe Lesot : orcid.org/0000-0002-5811-7530
- Philippe Berdagué : orcid.org/0000-0002-3430-921

Introduction

Is there a relationship between enantiomeric preference and isotopic fractionation of carbon-13? Asking this fundamental question in relation to a signature of the fractionation of carbon-13 or better with a position-specific ^{13}C isotopic redistribution (intramolecular fractionation) is to address some intriguing issues such as: i) the multiple factors inducing enantioselective isotopic effects; ii) the possibility of distinguishing between an abiotic and a biotic process during enantioselective degradations; iii) the possible authentication of molecules naturally occuring in plants thanks to the specific enantioisotopomeric excesses (*eie*'s); and iv) better understand the origin of the specific homochirality of bioproducts [**1, 2, 3**]. Indeed, in terms of homochirality, Nature is highly enantioselective, and it is questionable why certain classes of natural chiral molecules such as sugars or amino acids (AA), for example, exist in nearly only one enantiomeric form, *L* or *D* [**4**].

Age estimation can be achieved from the racemization rates of the AAs [**5**], the criterion being that very old samples should show *D*/*L* ratios close to the racemization [**6**]. When the global isotopic content is considered, the isotope effects associated with all these phenomena are relatively weak because they are 'diluted' by the contribution of carbons far from the center of enantioselectivity [**7**]. During a remediation process, involving a biotic degradation process, enantiomeric fractionation can occur either by cellular uptake or by enzymatic transformation, whereas isotope fractionation is mainly expected if chemical bonds are altered in the enzymatic transformation but not during cellular uptake [**8**]. Therefore, if absorption is the limiting step, enantiomeric fractionation is expected but not isotope fractionation. As a corollary, if enzymatic reaction is the limiting step, then changes in enantiomeric and isotopic fractionation are expected. A much better view would be obtained by performing a position-specific isotope content determination in order to accurately study isotopic effects in relation to enantiomerism. In this context, NMR spectroscopy is the most appropriate modern tool to provide such intramolecular isotope analysis.

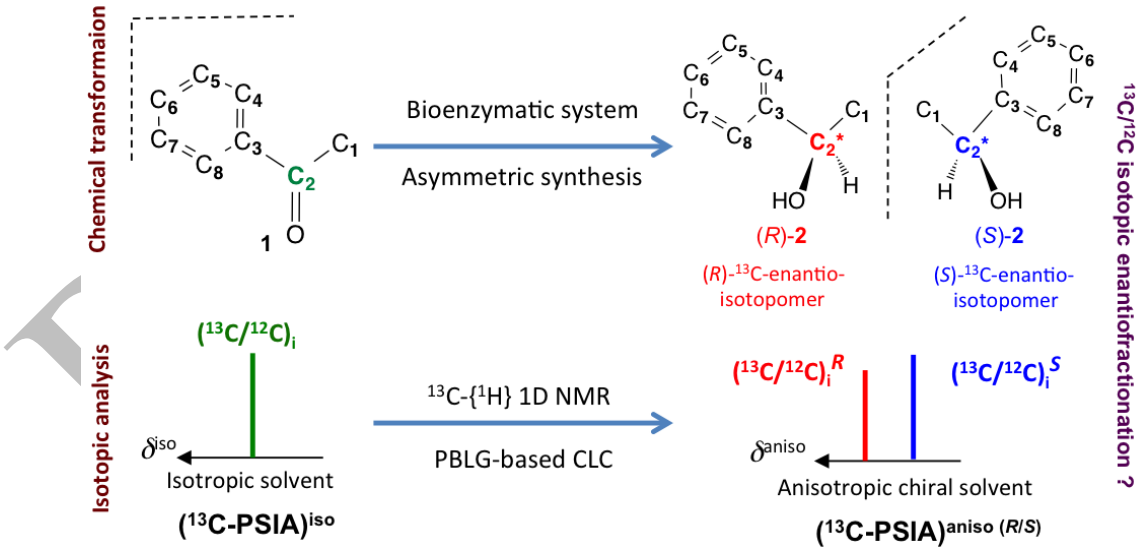

Figure 1. *Schematic description of the enantiomeric ^{13}C isotope fractionation phenomenon (enantiofractionation) in the case of the asymmetric reduction of the acetophenone (**1**) to 1-phenylethyl alcohol (**2**) and its possible experimental evidence using ^{13}C-(^{1}H} 1D NMR spectroscopy in presence of enantiopure external stimuli such as CLC's. The position of ^{13}C resonances and the peak intensities for the R and S isomers are arbitrarily defined.*

In this perspective/research article, we propose to experimentally evaluate the possibility to reveal possible effects associated with the enantiomeric position-specific ^{13}C isotope fractionation (EPSIF), using quantitative ^{13}C NMR-based strategies. For our purpose, we explore and describe isotropic and anisotropic ^{13}C NMR methodologies to investigate this intriguing phenomenon, never approached so far, to the best of our knowledge. The problem addressed here is highly challenging for two reasons: i) the possibility to spectrally discriminate enough the ^{13}C NMR signals of stereogenic center and also ^{13}C around it for each enantiomer and so to avoid problem of peak overlapping; ii) the ability to record ^{13}C-{^{1}H} spectra with sufficiently high signal-to-noise ratios to meet the required permil precision (‰) in isotope analysis and hence to accurately determine the $^{13}C/^{12}C$ isotope ratio", despite the doubling of ^{13}C signals due to the enantiodiscrimination. From a more practical viewpoint, we will examine potential sources of errors that can affect the robustness of anisotropic ^{13}C isotopic measurements within short- and long-term repeatability.

As illustrative example, we focus our attention to the ^{13}C isotopic analysis of a model chiral molecule of low molecular weight (122.16 g.mol^{-1}) the 1-phenylethyl alcohol (**2**) (see **Fig. 1**). Chemically, this simple aromatic alcohol can be obtained by the asymmetric reduction of the acetophenone (**1**) (a prochiral substrate) using either biological processes (enzymatic catalysed reaction) or synthetic transformations as schematically depicted in **Figure 1** [**9, 10, 11**]. Due to kinetic and/or equilibrium isotope effects, isotope fractionation of ^{13}C is possible, which would result in different EPSIFs for (*R*)-**2** and (*S*)-**2**. Typically, after a conversion of the order of 10 to 20%, the isotopic fractionation could be experimentally demonstrated and lead to the calculation of a position-specific enrichment factor, ε_i, associated with the chemical process followed [**7**].

Questions and analytical challenges

Chirality and naturality

Proteins are essentially composed of *L*-amino acids. *D*-amino acids are naturally rare but can be the result ofunusual or artificial transformations or derived from the abiotic racemization of the *L*-amino acids [**12**]. A large part of *D*-form is found in the soil due to bacterial activity [**13**]. For example, alanine racemase is an important enzyme in the synthesis of bacterial cell walls [**14, 15, 16**].. It catalyses the interconversion of *L*- and *D*-alanine using pyridoxal phosphate (PLP) as a cofactor [**17, 18**]. However in plants, the metabolism of molecules used in flavours (aroma, essential oils, etc.) does not show this systematic selectivity for one enantiomer. Both enantiomers exist depending of the plant origin, leading to different odour/flavour for each enantiomer. The enantioselectivity study by chiral chromatography is now a well-known methodology to confirm the authenticity of the natural origin of a given molecule [**19, 20**].

Isotope signature

To explain the prevalence of the *L*-form of amino acids, it is accepted that the initial presence of a very slight enantiomeric imbalance and the amplification of chirality are necessary for the production of highly enantio-enriched amino acids [**21**]. Thus, it has been reported that chiral induction can be initiated by small amounts of an isotope (replacement by its ^{2}H, ^{13}C or ^{15}N isotope of a substituent on a prostereogen carbon atom), by the spontaneous

formation of enantiomeric excesses in the natural abundance of stable isotopes (*eie's*) [**22, 23**]. Since the enantiomeric ratio in flavouring molecules depend of its origin, this parameter is not sufficient alone to authenticate the product. Addition of isotope profiles for each enantiomer is usually decisive [**24**].

In the remediation of a chemical contamination, if the chemical is chiral but is used as racemates (very often the case for active molecules: pesticides, drugs, etc.), some microorganisms show enantioselective degradations. This means that one enantiomer degrades faster than the other, either because of preferential microbial absorption (ingestion) or because of preferential enzymatic activity. Studies have shown that all cases can be found: i) enantiomeric fractionation with no ^{13}C isotope fractionation, ii) significant ^{13}C fractionation with no enantiomeric selection, and iii) both enantiomeric and isotopic fractionation (See next paragraph).

Methods for $^{13}C/^{12}C$ isotope ratio determination

$^{13}C/^{12}C$ isotopic ratio measured by mass spectrometry (irm-MS, knows also as IRMS: Isotope Ratio Mass Spectrometry) [**25**] has been explored in first to investigate the issue of the enantiomeric isotopic fractionation [**3, 8, 26, 27, 28, 29, 30, 31, 32, 33, 34, 35**]. However, only the global (or average) isotope composition is accessible. The lack of position-specific $^{13}C/^{12}C$ isotope data led to a difficult analysis and interpretation of the results, making it impossible to unambiguously prove the existence of a ^{13}C fractionation effect, since concomitant inverse and normal effects may occur [**36**].

Based on proton-decoupled ^{13}C NMR (^{13}C-{^{1}H} NMR) spectroscopy, the isotropic ^{13}C-position-specific isotope analysis named irm-^{13}C NMR (isotope ratio measured by NMR) is now a well-established tool for the determination of intramolecular ^{13}C isotopic composition ($\delta^{13}C_i$) with appropriate precision of the order of 1‰ [**37**]. Irm-^{13}C NMR is capable of providing key ^{13}C isotopic data for the understanding of reaction mechanisms of (bio)chemical transformations [**38, 39, 40, 41**]. Nevertheless, this method alone does not allow a direct access to enantiomeric ^{13}C isotopic data associated to a pair of mirror-image isomers. To reach this aim, two approaches can be considered [**42, 43, 44**]: i) a physical separation of each enantiomer prior to their irm-NMR analysis; ii) an *in-situ* spectral enantiodiscrimination in presence of a chiral (enantiopure) stimuli.

Enantiodiscriminating ^{13}C-{^{1}H} NMR approaches

The use of standard irm-^{13}C NMR methodology to access to any enantiomeric ^{13}C isotopic data is only possible if mirror-image isomers are first physically separated [**42**]. Such a separation can be obtained by preparative chiral chromatography, for instance [**43**]. The success of this two-step strategy lies primarily on the use of an adequate chiral column as well as a robust optimisation of experimental conditions.

When physical separation of enantiomers is not desired or experimentally impossible, several alternatives exist. All lies on the same principle, and are based on the creation of diasteroselective interactions with an enantiopure agent (a chiral partner) because NMR technique alone is blind to enantiomers. In practice, combined with isotropic NMR, three types of enantiopure agents can be employed: i) chiral derivatizing agents (CDAs, known as Mosher's agents) which form covalent bonds with enantiomers and convert them into stable diastereoisomers; ii) chiral lanthanide-induced shift reagents (CLSRs) such as chiral europium (III) complexes, which are coordinated by the

enantiomers and lead to the formation of diastereoisomeric complexes; and iii) chiral solvating agents (CSAs) as Pirkle's agents or chiral cyclodextrines [**42, 43, 44**]. An alternative to these "isotropic" methods consists of using chiral aligning solvents such as chiral liquid crystals (CLC) that are

able to orient enantiomers differently on average. This differential orientational order leads to distinct order-dependant NMR observables for each enantiomer as the residual dipolar coupling (RDC), the residual chemical shift anisotropy (RCSA) or the residual quadrupolar coupling (RQC) for spin $I > 1/2$ [**45, 46, 47**].

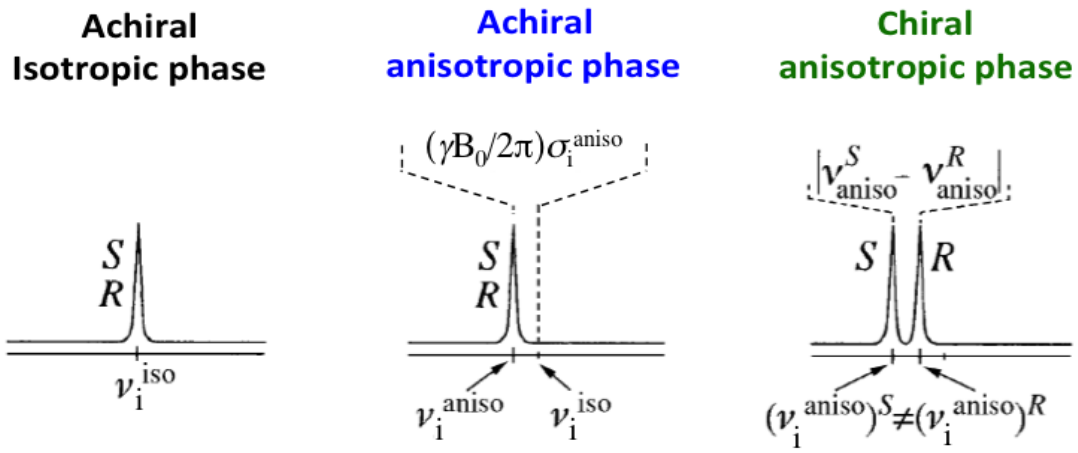

Figure 2. *Schematic description of the enantiodiscrimination in CLCs based on a difference of ^{13}C-RCSAs, $\Delta\nu_i = |\nu_i^{aniso} - \nu_i^{iso}|$. Disregarding any solvent effects (associated with the nature of the phase, isotropic or anisotropic), the frequency difference, $|\nu_i^{aniso} - \nu_i^{iso}|$ is equal to the quantity $(\gamma_i B_0/2\pi)\sigma_i^{aniso}$. The S and R assignments shown are arbitrary and spectral patterns are not plotted to scale.*

Obviously, each strategy possesses specific analytical advantages and drawbacks in terms of practicality and/or application ranges. In particular, for CDA-, CLSR- and CSA-based NMR methods, the enantiopure agent must be carefully chosen accordingly to the (specific) chemical functions of the investigated chiral compound. With the exception of cyclodextrins (chiral macrocycles), these agents are often not suitable for apolar chiral compounds. Interestingly, CLC-based NMR appears to be a very competitive alternative, much more universal than other NMR methods because the enantiodiscrimination mechanisms are strongly governed by the molecular shape recognition phenomenon, unlike the CLSR [**46, 47**].

Specificities of the anisotropic ^{13}C NMR

In this original approach, the distinct interactions of *S* and *R*-isomers with the enantiopure aligned molecules of the CLC (diastereomorphous interactions) in the NMR magnetic field results in their different average orientations as described by the Saupe's order matrix, $S_{\alpha\beta}^S$ and $S_{\alpha\beta}^R$, [**46, 47**]. This differentiated alignment leads to spectrally discriminate enantiomers on the basis of a difference of the residual chemical shift anisotropy (RCSA), residual dipolar coupling (RDC) and residual quadrupolar coupling (for spin $I > ½$) [**47**].

In oriented solvents, the electronic shielding constant of a carbon-13 atom *i* contains both an isotropic, σ_i^{iso}, and an anisotropic term, σ_i^{aniso}, (^{13}C-RCSA). This second contribution is generally different for a par of enantiomers

dissolved in CLCs. Thus, the respective resonance for the *R* and *S* isomers frequencies (in Hz), ν_i^R and ν_i^S, can be written as [**45, 47, 48**]:

$$\nu_i^{R \text{ or } S} = \frac{\gamma}{2\pi}\left(1 - \sigma_i^{iso} - \sigma_i^{aniso\,R \text{ or } S}\right) B_0 \quad \textbf{(1)}$$

where γ is the gyromagnetic ratio of ^{13}C nuclei. In fact, spectral separations only originate from the order parameter differences (S^R or S^S) involved in the term σ_i^{aniso} ($\sigma_i^{iso\,R} = \sigma_i^{iso\,S}$). A Schematic description of the enantiodiscrimination in CLCs based on a difference of ^{13}C-RCSAs is presented in **Figure 2**.

The development of this term (see Eqs. **SI-3** to **SI-6** in SI) shows that all factors increasing either the difference in order parameters between (*R*)- and (*S)*-isomer or the electronic shielding anisotropy of a given nucleus i (such as the hybridization state of carbon atom and the nature/electronegativity of the substituents bounded to it or to the adjacent nucleus) will increase the magnitude of σ_i^{aniso}. Thus if the magnitude of shielding anisotropy is rather small for sp^3 carbon-13 nuclei, significant ^{13}C-RCSAs can be obtained for sp and sp^2 carbon-13 nuclei [**48**]. In addition, the stronger the magnetic field, the better the spectral enantiodiscrimination effect (see **Eq. 1**).

In practice, anisotropic ^{13}C-{^1H} 1D NMR in CLCs is a robust tool, rather easy to implement on any routine NMR spectrometers. Similarly to isotropic NMR, recording anisotropic ^{13}C-{^1H} NMR spectra with high-field NMR spectrometers and possibly equipped of cryogenic probes [**49, 50**] is both advantageous in terms of spectral resolution (see **Eq. 1**) and sensitivity.

Materials and methods

Material and sample preparation

1-Phenethyl alcohol, organic co-solvant, and PBLG polymer were purchased from Sigma Aldrich, and used without further purification. The degree of polymerization (number of polypeptide units) is equal to 710. Co-solvant was, however, dried on molecular sieve before its use.

Samples of (*R/S*)-**2** (Aldrich P13-800) prepared during the preliminary step and recorded on a 9.4 T Avance III NMR spectrometer equipped with a 5-mm TBI (HCX) classical probe ($\nu_0(^{13}C)$ = 100.1 MHz)) were prepared using : i) ~100 mg of analyte, ii) ~ 150 mg of PBLG (m_{PBLG}/m_{Tot} = ~21.5%), iii) ~ 450 mg of co-solvent ($CHCl_3$ and CCl_4), The ratio (m_{PBLG}/m_{Tot}) is equal to 21.8% for sample ***AS-1***. A scalemic mixture (ee(*S*) = 40%) were also prepared to assign the absolute configuration of ^{13}C signals. Details are given in **Table SI-3**.

Polypeptide/chloroform-based oriented samples used for quantification purposes and recorded on a 16.5 T Avance III NMR spectrometer equipped with a 5-mm QCI (HFCN) cryogenic probe ($\nu_0(^{13}C)$ = 176.09 MHz) were prepared with : i) ~50 mg of *R*-(**2**) (Aldrich 685828) or *S*-(**2**) (Aldrich 05512-25G-F) and ~50 mg (*R*) + ~50 mg (*S*) analyte (racemic mixture prepared by weighing), 175 ± 1 mg of PBLG and ~540 mg of $CDCl_3$ (see **Table SI-5** for exact mass). The ratio (m_{PBLG}/m_{Tot}) for enantiopure and racemic mixture are equal to 21.4%. Compared to the previous samples, the larger amount of PBLG and chloroform used for isotopic measurements is justified in order to eliminate sample “edge effects” incompatible with a robust isotopic quantification as well as the longer length of the ^{13}C coil of the 5 mm cryoprobe (compared to the conventional probe), while the (m_{PBLG}/m_{Tot}) ratio is similar to that of

the samples tested in the preliminary stage. Also note that using $CDCl_3$ instead of a mixture ($CHCl_3$ and CCl_4) does not radically change the orientation behaviour of solute in terms of ^{13}C-RSCA-based enantiodiscriminations (variation of ± 1 Hz), whereas the anisotropic samples can be locked during the ^{13}C experiments (see below).

To reach the optimal spectral resolution, several cycles of centrifugation at low speed (500 rpm) of the (sealed-fire) NMR tubes were performed to remove concentration gradients along the sample. This operation is crucial because a macroscopic inhomogeneity (generated by matter concentration gradient) strongly increases the linewidths, and therefore reduces the SNR for solute signals. Other NMR details and preparation of NMR tubes are given in **SI**, and in previous refs [**46, 47, 48**].

Evaluation of ^{13}C longitudinal relaxation times

The determination of the ^{13}C longitudinal relaxation time $T_1(^{13}C)$ for each carbon of the analyte is an important data to determine the recycling delay, T_R, between two successive scans added in order to record spectra under robust quantitative conditions. For isotopic quantification purpose by irm-^{13}C NMR, it is recommend to use $T_R = 10 \times T_1(^{13}C)$ [**51**]. The classical inversion-recovery experiments was used to determine the $T_1(^{13}C)$ [**52**].

Quantitative ^{13}C-{^{1}H} experiments

For all quantification evaluations by ^{13}C-{^{1}H} NMR (isotropic and anisotropic), proton signals are only decoupled during the signal acquisition (inverse-gate pulse scheme) to minimize the nuclear overhauser effect (nOe) induced by the ^{1}H composite-pulse decoupling sequence (^{1}H-CPD). Regardless of the solvent used, identical data processing was applied: i) ^{13}C-{^{1}H} spectra were zerofilled to 128 k datapoints, and an exponential window function inducing a line broadening of 1.7 Hz (isotropic samples) and 1 Hz (anisotropic samples) was applied to the FID prior to FT, ii) a careful phase correction followed by an appropriate polynomial baseline correction by "parts" was then applied before any spectral deconvolution of resonances.

Areas of ^{13}C peaks corresponding to different carbon sites of the *R*-, *S*- and *R*/*S*-mixture in anisotropic phase were determined by the curve-fitting process implemented within Perch (Perch NMR Software, University of Kuopio, Finland [**53**]). Each resonance was smoothed by adjusting its chemical shifts, its amplitude, its width at half maximum (FWHM), its phase, and using a Lorentzian shaped lines including a Gaussian percentage. The peak areas measured in quantitative ^{13}C-{^{1}H} 1D-NMR spectra were corrected for accounting to the presence of ^{13}C-^{13}C isotopologues in the molecule, which gives rise to satellite lines.Finally, reduced molar fractions f_{iR} were calculated for the C-1, C-2, C-3, C-4/8, C-5/7, C-6 sites of analyte according to **Eq. 2** (see also **Table SI-1**):

$$f_{iR} = \frac{S_i}{(F_i \times S_T)} \qquad (\mathbf{2})$$

where S_i is the corrected peak area for position i, and S_T is the sum of the peak areas of all the measured sites. F_i is the statistical molar fraction of site i. In compound 2, this value is equal to 1/8 for C-1, C-2, C-3 and C-6 sites, and 2/8 for C-4/8 and C-5/7 sites (see also **Table SI-1**). From f_{iR} using the global value for δg (in ‰) obtained by irm-EA/MS, the δ_i (in ‰) for each NMR peak can be calculated according to ref [**54**]. Then the position-specific carbon

composition for each carbon i are expressed as $\delta(^{13}C_i)$ in ‰. It should be noted that these values were not calibrated according to the response factor of the spectrometer.

It is important to note that compared to the analysis in an isotropic solvent where only the analyte and solvent signals are observed (ignoring impurities from the solute/solvent), the analysis of the ^{13}C signals of solute in the PBLG phase may be more challenging. Indeed we observe ^{13}C peaks from the flexible side chain of the polypeptide that cannot be considered as simple artefacts (see **Figure 4** and **Fig. SI-4**). Due to the difference in dynamics between the solute and polymer (backbone and side chain), these additional PBLG ^{13}C signals are broader (and so weaker) than the analyte signal ($T_{2_{PBLG}}^{aniso} << T_{2_{solute}}^{aniso}$). In case of **2**, the proximity of these broad signals (*e.g.,* labeled peaks 2, 6 and 8) can be a source of error for an accurate determination of the area of the nearest enantiomer peak (here (*R*)-peak for C-2, (*S*)-peak for C-3 and (*R*)-peak for C-1). Examination of their impact on the measurement of peak areas and hence on the accuracy of $\delta(^{13}C)$ values is presented in the discussion section.

Irm EA/MS: global stable-isotope analysis

Global carbon ($^{13}C/^{12}C$) isotope ratio measurements, expressed in delta notation, $\delta^{13}C_g$ (‰), was determined by isotope ratio monitoring by mass spectrometry (irm-MS) using an Integra2 spectrometer (Sercon Instruments, Crewe, UK) linked to a Sercon elemental analyser (EA) fitted with an autosampler (Sercon Instruments, Crewe, UK). About 1 mg of sample was sealed in a tin capsule (4 × 6 mm Sercon tin capsule). $\delta^{13}C_g$ of the resulting gases, CO_2 was determined by reference to a working standard of glutamic acid standardized against international reference material (IAEA-CH7 for carbon isotope ratio).

The ^{13}C global (or average) isotope compositions of the whole molecule were calculated from:

$$\delta_g(per\ mil) = \left(\frac{R}{R_{std}} - 1\right) \times 1000 \qquad (\mathbf{3})$$

where R is the isotope ratio of the sample and R_{std} is the isotope ratio of Vienna PeeDee Belemnite reference standard (V-PDB) for ^{13}C (R_{std} = 0.0112372) [**55, 56**].

Results and discussion

Quantification requirements and optimization of anisotropic samples

The quality/robustness of quantitative ($^{13}C/^{12}C$) ratio measurements by anisotropic 176.09 MHz ^{13}C NMR using lyotropic polypeptide-based CLCs as solvents mainly depends on two factors: i) the SNR for each ^{13}C peak, ii) the FWHM ($\propto 1/T_2^*$), and iii) the magnitude of separations for the enantiodiscriminated inequivalent ^{13}C sites [**47,48**]. These three factors are closely related to the proportion of the sample components (solute/polymer/co-solvent), the nature of polypeptide, and the co-solvent polarity; each of them affects the mesophase viscosity as well as the enantiodiscrimination mechanisms. Generally for aromatic alcohols as analyte **2**, PBLG mesophases prepared with weakly-polar organic solvents (as chloroform, μ = 1.04 D) or a mixture (chloroform and tetrachloromethane) provides good results in terms of sample fluidity and enantiodiscriminations [**57**].

To reach the permil precision desired in irm-^{13}C NMR, a significant quantity of solute is needed to obtain an expected minimal SNR ≥ 500 within a reasonable experimental time to avoid magnetic drifts (90 - 120 min). In case of **2**, 50 mg (4.10^{-5} mol) *per* enantiomer appear sufficient (at 17.5 T) when FWHM < 3 Hz.

Advantage of using deuterated co-solvents

Interestingly, the use of $CDCl_3$ as deuterated organic co-solvent is advantageous for two reasons. First of all, the high sensitivity of the ^{2}H quadrupolar interaction, can easily reflecting possible gradients of order ("disorder of order") of the liquid-crystalline phase [**58**], thus providing a simple way for a robust evaluation of its homogeneity. In clear, the observation of a ^{2}H doublet showing large intensity difference between both components indicates a non-ideal situation. In practice, a new series of sample centrifugations is recommended. The presence of dissymmetrical ^{2}H lineshapes clearly indicates an inadequate magnetic homogeneity that should be corrected by re-shimming the magnet. One example of ideal ^{2}H 1D spectrum for $CDCl_3$ oriented in PBLG is shown in **Fig. SI-2a**. Generally, ^{2}H spectrum of good spectral quality leads to excellent ^{13}C-{^{1}H} spectra. Second, we can lock the magnetic field of the spectrometer during the ^{13}C-{^{1}H} NMR experiments on the frequency of one of components of the ^{2}H quadrupolar doublet of $CDCl_3$, either the shielded or deshielded peak. However it is not recommended to apply any procedure of autoshimming during a series of experiments. Indeed, the majority of attempts using the autoshimming procedure, during the acquisition, led to a loss of significant magnetic homogeneity over time incompatible with irm-^{13}C NMR measurements.

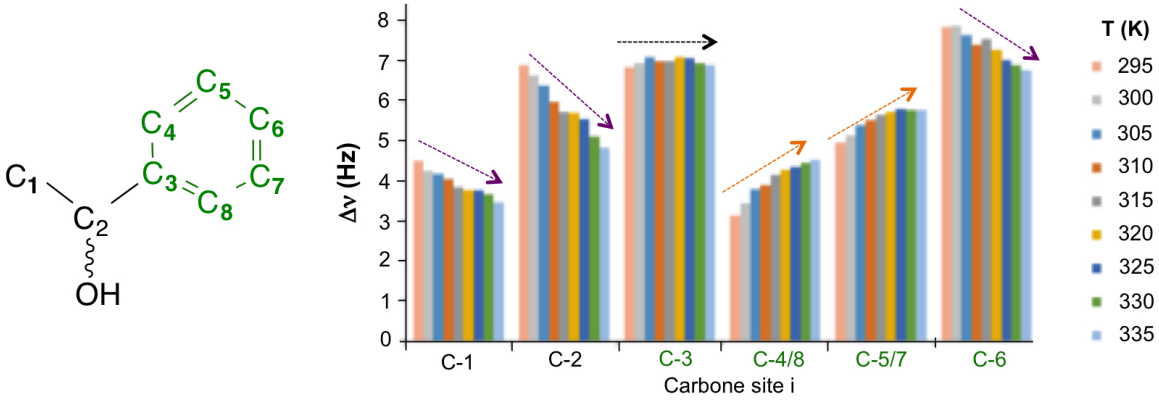

Figure 3. *Variation of $\Delta\nu(^{13}C_i)$ expressed in Hz for each inequivalent carbon site of **2** (**AS-1**) between 295 and 335 K, and measured at 9.4 T ($\nu(^{13}C)$ = 100.3 MHz).*

Temperature and consequences

Changing the sample temperature (T) is a valuable option to vary the ^{13}C-RCSA contribution ($\sigma_i^{\text{aniso}\,S\text{ or }R}$) for each inequivalent carbon site, and hence modify the spectral enantiodifferences ($\Delta\delta$ (in ppm) or $\Delta\nu$ (in Hz)) measured on ^{13}C NMR spectra when a racemic/scalemic mixture is used. Expressed in Hz, this difference is equal to:

$$\Delta\nu_i = \left|\nu_i^S - \nu_i^R\right| = \left|\frac{\gamma}{2\pi}\left(\Delta\sigma_i^{\text{aniso}}\right)B_0\right|. \quad (4)$$

As seen in **Figure 3,** the variation of $\Delta\nu_i$ $(\propto \Delta\sigma_i^{aniso})$ for each ^{13}C site as a function of T may be different (increase or decrease) according to the ^{13}C site of **2.** Thus, we can note that $\Delta\delta$ values decreases with T for C-1, C-2 and C-6 atom sites, increase for C-4 and C-5 while remains more or less constant for C-3. These divergences originate from the complex combination (toward order parameters, *S*) of terms contributing to σ_i^{aniso} (see Eqs. **SI-4** to **SI-6**), and in turn to the observed differences, $|\Delta\sigma_i^{aniso}|$. The great versatility of term $\Delta\sigma_i^{aniso}$ relative to molecular order makes the variation of $\Delta\nu_i$ as a function of T very unpredictable (at least when the variation of T does not exceed 30 - 40 K).

As with isotropic NMR, the temperature of the sample significantly influences the anisotropic longitudinal relaxation times of the carbon atoms ($T_1(^{13}C)^{aniso} < T_1(^{13}C)^{iso}$). This can have a significant impact on the overall experiment time, T_{exp}, when ^{13}C-{^1H} spectra are recorded under quantitative conditions (see above). In practice, the choice of the optimal sample temperature must result from a reasonable balance between $\Delta\nu$(*R*/*S*), FWHM, T_R, T_{exp} and the SNR. Given the composition of the sample selected for **2**, a good compromise is obtained at T = 303 K, thus leading to the longest $T_1(^{13}C)^{aniso}$ = 5.8 sec value for C-3 (value to be compared to $T_1(^{13}C)^{iso}$ = 11.4 sec), and a experimental time of a little more than 2 hours (T_{exp} = 124 min, T_R = 61 sec, with t_{aq} = 1 sec) for 4 dummy scans and 120 scans added. **Table 1** lists all relevant ^{13}C spectral data for **2** at 303 K.

Choice of the ^{1}H-CPD scheme

Last, but not least, in irm-^{13}C NMR, the accuracy of ^{13}C-{^1H} NMR measurements depends on the quality of the ^1H-CPD decoupling type used [**59, 60**]. In a preliminary step, two ^1H-CPD schemes were tested and compared: the well-known Waltz-16 [**61**] and the recommended (adiabatic) scheme pulse denoted X4 for irm-NMR [**62**] (see **Figure SI-4)**. The analysis of experimental results in oriented solvents points out that the X4 ^1H-CPD scheme gives more repeatable and reproducible isotopic measurements compared to the Waltz-16 scheme. This observation confirms the previous request for isotropic irm-NMR analysis [**63**]. Beyond the adiabaticity of X4 decoupling, this scheme eliminates more efficiently the large spin-spin total couplings, $T(^{13}C\text{-}^1H) = J(^{13}C\text{-}^1H) + 2D(^{13}C\text{-}^1H)$, associated with C-H pairs in PBLG and minimizes the second-order effect met with strongly coupled ^1H-^1H spin systems. This leads to the observation of sharper ^{13}C signals for the PBLG (see **Fig. SI-4a**), in particular at the terminal (aromatic) carbonatoms of the side chain which are highly mobile with respect to the peptide backbone. This situation is very favourable for a more reliable deconvolution of the analyte signals, especially when they are close to the polymer signals. A typical example of quantitative anisotropic ^{13}C-{^1H} 1D spectrum obtained for (*R*/*S*)-**2** recorded in nearly two hours (T_R = 61 s, number of scans = 120, dummy scans = 4) and using the X4 decoupling scheme is shown in **Figure 4**. As seen all inequivalent carbon sites are spectrally enantiodiscriminated on basis of ^{13}C-RCSA differences (see **Table 1**).

Table 1. Spectral ^{13}C data of all C-1 to C-8 carbon sites of (*R*)-**2**, (*S*)-**2** and (*R*/*S*)-**2**, measured at 303 K and 17.5 T

Data	Carbon site					
Atom	C-1	C-2	C-3	C-4/8	C-5/7	C-6
Type	CH_3	C*-H	Cq	2×CH	2×CH	CH
Hybrid	sp^3	sp^3	sp^2	sp^2	sp^2	sp^2
$\delta(^{13}C)^{iso}$ a, c	25.04	70.24	145.78	125.33	128.39	127.34
$\delta(^{13}C)^{S}$, aniso b, c	24.91	69.71	146.25	125.44	128.34	127.47
$\delta(^{13}C)^{R}$, aniso b, c	24.95	69.65	146.32	125.47	128.39	127.54
$\Delta\nu(^{13}C)^{R/S\ aniso}$ d	7.0	10.5	11.7	6.2	8.8	13
FWHM[e]	2.8	2.8	2.7	2.9	2.7	2.9
$T_1(^{13}C)^{iso}$ f	3.4	8.6	11.4	6.5	6.3	4.9
$T_1(^{13}C)^{aniso}$ g	1.9	4.0	5.8	3.2	3.1	2.3
SNR^{iso} h	760	750	830	1620	1610	790
SNR^{aniso} i	700	640	710	1470	1460	710
SNR^{aniso} j	540	520	560	1130	1120	540

[a] $\delta(^{13}C)$ in ppm of (±)-**2** in isotropic phase ($CDCl_3$). [b] $\delta(^{13}C)$ in ppm of (*S*)-**2 or** (*R*)-**2** in PBLG/$CDCl_3$. [c] The central ^{13}C resonance of $CDCl_3$ in isotropic and anisotropic phase is calibrated at 77.0 ppm. [d] $\Delta\nu(^{13}C)$ is equal to $|\nu(^{13}C)^{R} - \nu(^{13}C)^{S}|$ (in Hz). [e] FWHM in Hz: full with at half maximum (average value) measured in the CLC. [f] Isotropic longitudinal relaxation time $T_1(^{13}C)$ in sec for (*S*)-**2**. [g] Anisotropic longitudinal relaxation time $T_1(^{13}C)$ (average value of enantiomers). [h] SNR measured for (*S*)-**2** in isotropic phase. [i] SNR (no unit) measured for (*S*)-**2** in anisotropic phase. [j] SNR measured for (±)-**2** (average value of *R* and *S* signal).

Short- and long-term repeatability of anisotropic ^{13}C-{^1H} NMR experiments for the enantiopure oriented samples

Given the small isotopic variations expected, the ability to evaluate possible effects of enantiomeric isotope fractionation is highly dependent on the ability of the method to obtain precise data. In this section, we first examined and compared the precision of the ^{13}C isotope measurements obtained in the case of the enantiopur samples, (*R*)-**2** and (*S*)-**2**, in anisotropic solvent (***AS-3*** and ***AS-4***) in terms of short- and long-term repeatability. In **Figure SI-4**, the anisotropic ^{13}C-{^1H} 1D spectrum of (*S*)-**2** is presented and can be compared to that of **Figure 4**.

Short-term repeatability of anisotropic ^{13}C NMR experiments for (*S*)-**2** and (*R*)-**2** samples has been assessed by calculating the standard deviation, $SD(^{13}C)_i$, for each inequivalent carbon site and using seven replicates (all numeric data are given in SI, see **Tables SI-8, SI-10, SI-11**). Long-term repeatability was evaluated by recording two series of independent experiments (S-I and S-2) separated by a period of ~70 days (recorded on the same instrument). **Figures 5a**,**b** show the variation of ^{13}C isotopic compositions, $\delta^{13}C_i$, in ‰ *versus* the six inequivalent ^{13}C sites of (*S*)-**2** and (*R*)-**2**, respectively, both calculated for each series (S-I and S-II) of seven consecutive NMR experiments (7 replicates) and the associated average value must result from a reasonable balance between various parameters: $\Delta\Delta\nu$, FWHM, T_R, T_{exp} and the SNR. Given the composition of the sample selected for **2**, a good compromise is obtained at T = 303 K, thus leading to the longest $T_1(^{13}C)^{aniiso}$ value for C-3 of 5.8 sec, and experiment with T_{exp} 124

minutes for 4 dummy scans and 120 scans added. **Table 1** lists all relevant ^{13}C spectral data for **2**. Additionally, **Figure 5c** graphically details the variation of $SD(^{13}C)_i$'s for each isomer of the two series. Note that column plots for each isomer is also proposed in Supp. Info. (**Figs. SI-5** and **SI-6**). Examination of data reveals that the $\delta^{13}C_i$ values for both enantiomers follow the same trends (from -20‰ to -86‰), even so some carbon site as a significant variation between enantiomers as observed with C-2 ($|\Delta\delta^{13}C_2|$ = ~40 ‰). As seen on plots, the *SD* values and their variations within each series are very similar, varying between 0.5 to 2.4 ‰ with an average value of SD's found at 1.27‰.

From the analysis of anisotropic enantiopure samples, (*R*)-**2** or (*S*)-**2**, two experimental facts can be drawn:

i) isotopic data show a good repeatability (over a series of 7 exp.) while the *SD* values are in the same range than for isotropic samples (< 2.5 ‰) with an average value of *SD*'s found at 1.17 ‰ (see **Table SI-12**),

ii) for the long-term repeatability, the results are very similar over a period of about 70 days, but it could be argued (case of (*R)*-isomer) that standards (used for isotropic samples) are not reached for a robust quantification of ($^{13}C/^{12}C$) ratio (see **Figs. SI-5 and SI-6**). Technically, reproduce the identical anisotropic spectra with oriented samples (even with fired-sealed NMR tube) is always more difficult than with isotropic samples,) due to possible tiny order variations

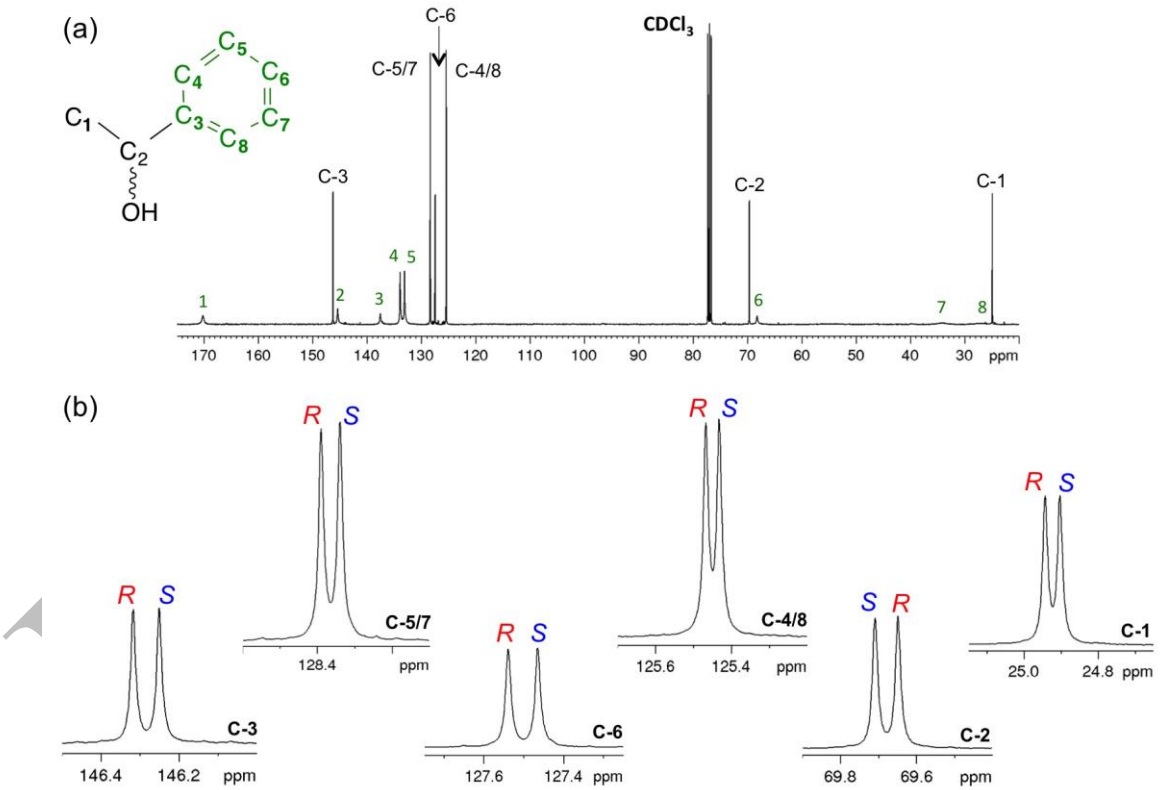

Figure 4. *(a) 176.09 MHz ^{13}C-{^1H} 1D NMR spectrum of (±)-**2** (**AS-5**) in the PBLG/$CDCl_3$ chiral mesophase at 303 K (T_{exp} = 124 min, 120 scans and 4 dummy scans, X4 decoupling scheme). An exponential filtering (LB = 1 Hz) is applied. ^{13}C-peaks labelled with a green number (1 to 8) originate from PBLG polymer side chain (see also **Figure SI-4**). Compared to the analyte ^{13}C signals, they are both smaller and larger ($T_2^{PBLG} < T_2^{Solute}$). (b) Zoom on each ^{13}C site. Spectra data are listed in **Table 1**. The R/S assignment was made by comparison with the ^{13}C-{^1H} spectra of (R)-**2** and (S)-**2** as well as the comparison with a scalemic mixture of **2** (ee(S) = 40% (**AS-2**)). Note the inversion of spectral positions for S and R isomers at the carbon site C-2 compared to other sites.*

(centrifugation step not always identical). Even small, these variations can affect the peak shapes and/or the position of ^{13}C satellites peak due to tiny variation of (^{13}C-^{13}C)-RDC values associated with adjacent pairs of ^{13}C-^{13}C isotopologues, and so modifying the final measurements of some permils. This occurrence does not exist with isotropic samples.

As mentioned previously, anisotropic ^{13}C-{^{1}H} spectra are featured by the presence of PBLG ^{13}C signals. To assess their impact on the deconvolution process of analyte signals in enantiopur samples, a new series of spectral smoothing including their deconvolution have been carried out. Isotopic data and associated plots are given in Supp. Information (see **Table SI-10 and SI-11** (for S-1 and S-II) and **Figs. SI-7** to **SI-10**).

The comparison of isotopic data with and without PBLG deconvolution for ***AS-3*** and ***AS-4*** indicates that the $SD(^{13}C)_i$ values for each site are very similar. Besides, excepted for the methyl C-1 (*R*-isomer), the $\Delta\delta(^{13}C)_i$ values range between +0.6 to -3 ‰ with an average value found at -0.4 and -0.3 ‰ for *R* and *S,* over the two series respectively. The largest difference, measured on C-1(*R*) located at 25 ppm, originates from the very close proximity of the broad ^{13}C signal of the CH_2 group of the side chain bonded to the C*H of the peptide unit; this effect being minimized for the signal of *S*-isomer located slightly further away (25.0 ppm) (see **Figures 4 and SI-4**). Same situation exists with the C-2 site of (*R*)-**2** compared to (*S*)-**2** (δ^{PBLG} = 68.1 ppm) as well as the C-3 site (δ^{PBLG} = 145.5 ppm) but with smaller $\Delta\delta^{aver}(^{13}C)_i$'s due to highest (sharper) PBLG peaks, thus enhancing the deconvolution process quality. In other words, the deconvolution of broad ^{13}C signals of PBLGs is necessary when their overlap with the sharper ^{13}C signals of the analyte is too important to be ignored, as in the case of C-1 site of (*R*)-**2** (-4 ‰) compared to (*S*)-**2** (-1.5 ‰).

Analysis of the anisotropic racemic mixture

In a third step, the anisotropic ^{13}C-{^{1}H} spectra of a racemic mixture of **2** (denoted (*R*/*S*)-**2**, sample ***AS-5***) prepared as an equimassic mixture of the pure enantiomers were recorded under quantitative conditions and examined. Compared to enantiopure oriented samples, the case of a racemic mixture but also of any scalemic mixtures (0 < *ee*(%) < 100) is spectrally more complex to analyse and deconvolute, mainly because the ^{13}C signals of the *R*- and *S*-isomers are expected to be spectrally enantiodiscriminated for each inequivalent carbon site, with spectral differences in Hz equal to 2 to 3 times the FWHM of analyte peaks.

In case of **2** in PBLG, these differences range for 6 to 12 Hz (see **Table 1**). To this doubling of the ^{13}C peaks (which results in a reduction of the SNR by a factor of 2), one must considered the presence of ^{13}C satellites, the impurities originating from each enantiomer, the instrumental artifacts and the PBLG signals. The experimental NMR conditions for evaluating the short- and long-term repeatability for ***AS-5*** is identical to those used with the oriented enantiopure samples. Hereagain two series of data (S-I and S-II, ~120 days, same instrument) with consecutive 7 replicates each was chosen, with a total experimental duration not exceeding 15 hours, mainly for avoiding possible mesophase homogeneity degradation over time. As previously, the smoothing process of analyte signals was performed with and without the deconvolution of ^{13}C signals of PBLG polymer, but have been adapted to the spectral complexity of ***AS-5***.

All $\delta(^{13}C)_i$ and $SD(^{13}C)_i$'s values for each enantiomer are reported in **Table SI-9** as well as in **Tables SI-12** and **SI-13** (for S-I and S-II, respectively). Column plots of $\delta^{aver}(^{13}C)$'s of (*R*)-**2** and (*S*)-**2** isomers in the racemic mixture (***AS-5***) are displayed in **Figure 6**. Additional associated graphs or column plots are reported in Supp. Info. (**Figs. SI-11** to **SI-13**).

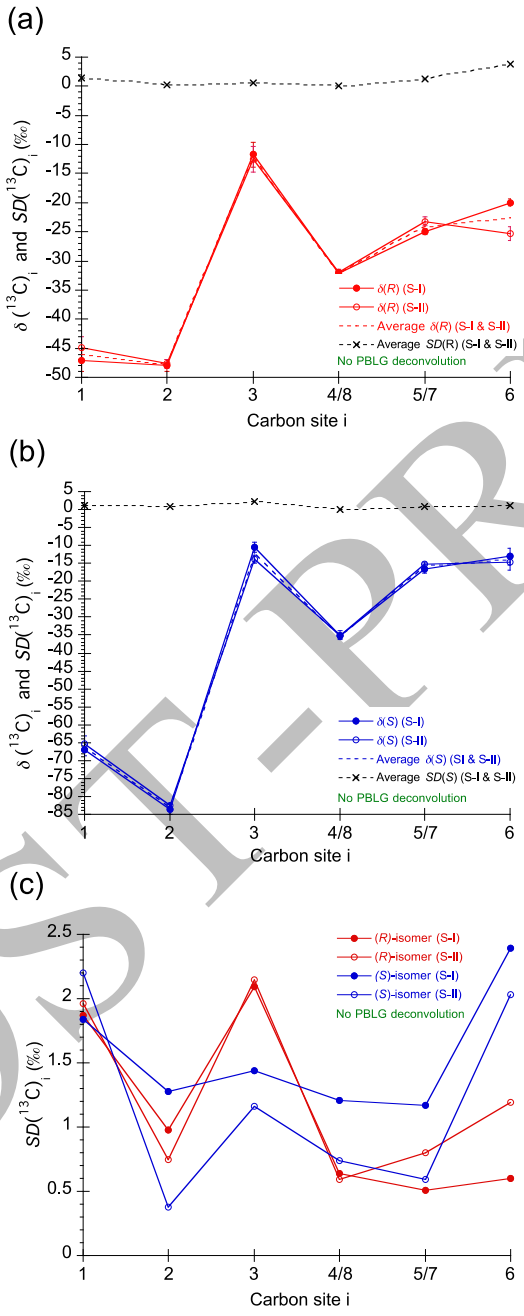

Figure 5. *(a and b) Variation of $\delta(^{13}C_i)$'s versus the six inequivalent ^{13}C sites of (R)- and (S)-isomers of **2** in anisotropic phase (samples **AS-3** and **AS-4**; series S-I and S-II; 7 replicates), as well as the $\delta^{aver}(^{13}C)$'s (red or blue dotted lines) and $SD^{aver}(^{13}C)$'s (black dotted line). (c) Variation of $SD(^{13}C)$'s of the S- (red) and R-enantiomers (blue) over the two series. The PBLG ^{13}C signals are not deconvoluted here.*

The analysis of short and long-term isotopic data extracted from (*R/S*)-**2** sample deserves a special attention. Compared to the ^{13}C isotopic measurements of the enantiopure samples, higher $SD^{aver}(^{13}C)_i^{R/S}$ values (up to ~9 ‰

instead of ~4 ‰), with an average value of ~3.9 ‰ instead of ~1.5 ‰) are obtained. From the point of view of isotopic compositions of (*R*)-and (*S*)-isomer, measured in enantiopure sample and in the racemic sample (see **Tables SI-8** and **SI-9**), the comparison of results shows that isotopic data follow the same trends, but some divergences are observed with an average difference of about 9 ‰ (see **Table SI-15**). These results are observed both without and with the deconvolution of PBLG signals. Several arguments can be given for explaining these discrepancies, oneassociated to the deconvolution protocol used, the other associated with the quality of NMR experiments.

With respect to the protocol, the use of reduced molar fractions, f_{iR}, can be considered as one of the main sources of error. While this approach avoids the use of an internal isotopic reference, but also the errors in the weighed mass of components of the sample, it is likely to accumulate errors in the δ□^{13}C)$_i$ values. In relation to NMR experiments, we can mention the following reasons:

i) as for enantiopure samples, but in a more pronounced way, broader anisotropic ^{13}C peaks lead to small SNR,

ii) on the racemic sample, the *R* and *S* signals are not completely separated ($\Delta\Delta\nu$ = 5 to 8 Hz) and the baseline does not return to zero between the two peaks. In this condition, a smoothing effect is applied

on the repeatability. *SD* value of 4, however, indicate that the experiment is sufficiently repeatable to differentiate between samples if the experiments are reproducible,

iii) compared to enantiopure samples, we can see that the presence of one, two or three pairs of ^{13}C satellites associated with each dedoubled peak (isotopologues ^{13}C-^{13}C) by enantiodiscrimination lead to a complex distribution of small peaks (satellites) at foot of "^{13}C intense signals" not easy to simply deconvolute (see **Fig. 7**),

iv) the difference of impurities associated with the samples of *R* and *S* isomers (different packaging) that are now simultaneously present in the racemic mixture can be cumbersome when a racemic mixture is prepared.

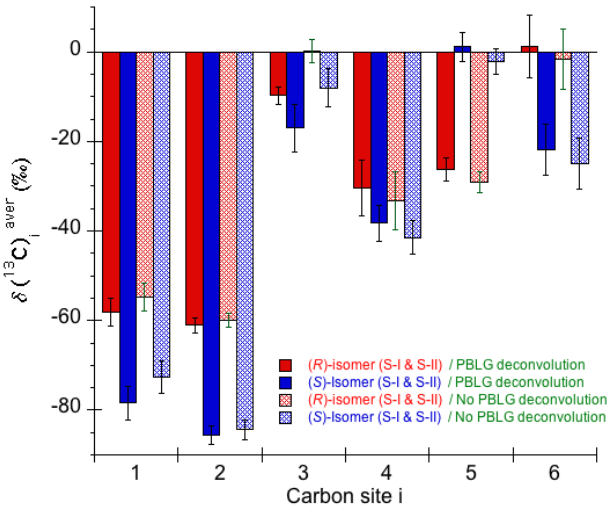

Figure 6. *Variation of $\delta^{aver}(^{13}C)_i$'s with the associated SD($^{13}C)_i$'s (both in ‰) of (R)-**2** and (S)-**2** isomer in the racemic mixture (**AS-5**) versus the six inequivalent ^{13}C sites) obtained with the experimental data series (S-I and S-II). Solid and shaded columns correspond to isotopic data obtained with or without PBLG deconvolution, respectively.*

Control of the long-term mesophase stability and homogeneity in anisotropic samples

Disregarding the various reasons presented above, we have identified that the major difficulties preventing the best repeatability of the irm ^{13}C-NMR experiments (the lowest *SD*) in anisotropic chiral solvents (compared to isotropic irm ^{13}C-NMR) is related to the long-term macroscopic stability of the liquid-crystalline solvent.

A simple criterion to evaluate the mesophase long-term instabilities, and *in fine* variations of the solute orientational order over time that is unsuitable for ^{13}C quantitative measurements, is the comparison of the ^{2}H-{^{1}H} signal of chloroform-d_1 before and after the series of ^{13}C spectra. If both ^{2}H spectra show significant spectral changes (such as significant variations of the line shapes symmetry, the changes in the maximum intensity of the components of ^{2}H-QD, or a mirror-image desymmetrisation of the ^{2}H-QD (see **Fig. SI-2b**), then the series should be considered suspect and potentially discarded for any quantitative purposes.

Associated with the long-term repeatability of anisotropic ^{13}C experiments, it is important to apply identical (or at least very similar) protocol (cycle of centrifugations speed, equilibrium time of the sample in the magnetic field of NMR spectrometer, …) before each new campaign of experiments. Here, again, the comparison of the ^{2}H-{^{1}H} signal of chloroform-d_1 through the magnitude of the $\Delta\nu_Q(^2H)$ is a good indicator of chemical stability of the mesophase (no degradation), as well as its similarity in terms of orientational organization.

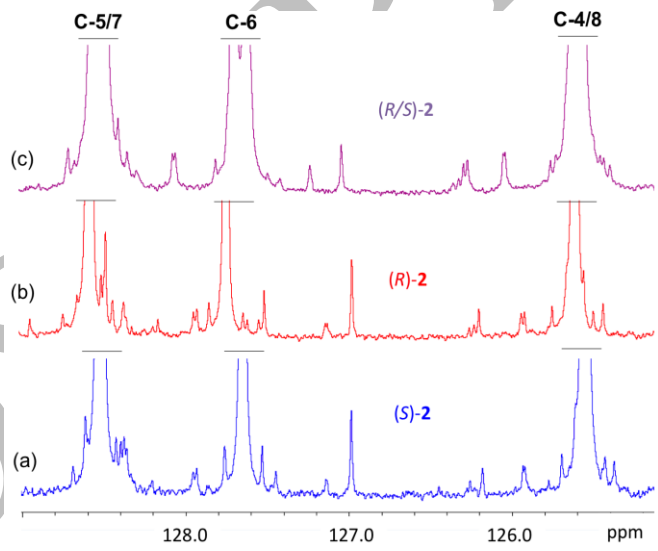

Figure 7. *Zoom on the C-4/8, C-5/7 and C-6 aromatic signals located in the region of 125-129 ppm of (a) (S)-**2**, (b) (R)-**2**, and (c) (R/S)-**2** showing both the different pairs of ^{13}C satellites associated with the adjacent isotopomers, but also solute impurities*.

Control of the long-term mesophase stability and homogeneity in anisotropic samples

Disregarding the various reasons presented above, we have identified that the major difficulties preventing the best repeatability of the irm ^{13}C-NMR experiments (the lowest *SD*) in anisotropic chiral solvents (compared to isotropic irm ^{13}C-NMR) is related to the long-term macroscopic stability of the liquid-crystalline solvent. A simple criterion to evaluate the mesophase long-term instabilities, and *in fine* variations of the solute orientational order over time that is unsuitable for ^{13}C quantitative measurements, is the comparison of the ^{2}H-{^{1}H} signal of chloroform-d_1 before and

after the series of ^{13}C spectra. If both ^{2}H spectra show significant spectral changes (such as significant variations of the line shapes symmetry, the changes in the maximum intensity of the components of ^{2}H-QD, or a mirror-image desymmetrisation of the ^{2}H-QD (see **Fig. SI-2b**), then the series should be considered suspect and potentially discarded for any quantitative purposes.

Associated with the long-term reproducibility of anisotropic ^{13}C experiments, it is important to apply identical (or at least very similar) protocol (cycle of centrifugations speed, equilibrium time of the sample in the magnetic field of spectrometer, …) before each new campaign of experiments. Here, again, the comparison of the ^{2}H-{^{1}H} signal of chloroform-d_1 through the magnitude of the $\Delta\nu_Q(^{2}H)$ is a good indicator of chemical stability of the mesophase (no degradation), as well as its similarity in terms of orientational organization.

Comparison of isotopic data with isotropic samples

Finally, the isotopic data, $\delta(^{13}C)_i$ and $SD(^{13}C)_i$ values, extracted from anisotropic samples (enantiopur and racemic) can be compared to that determined in isotropic phase (neat $CDCl_3$ at 303 K). Experimental data have been exploited using two series of five replicates. All numerical data obtained are given in Supp. Info. (see **Table SI-14)** as well as the associated graphs (see **Figures SI-14** and **SI-15**) and a comparative table (see **Table SI-15)**.

In an ideal case, the $\delta(^{13}C)_i$'s and SD $(^{13}C)_i$'s in isotropic and anisotropic phase should be in principle non-statistically different, in particular in the case of enantiopure sample, the case of racemic being more complex. As expected, SD^{aver} or all SD $^{13}C)_i$'s determined in isotropic enantiopur sample are smaller (~0.6 ‰) than in the anisotropic enantiopur sample (~1 ‰), mainly due to higher SNR for all carbon sites (smaller FWHM's). However, the two datasets are relative close, showing the reliability of quantitative ^{13}C-{^{1}H} NMR in anisotropic solvent. In terms of trueness, the comparison of $\delta(^{13}C)_i$'s shows experimental differences. Same reasons discussed previously can be also used for explaining the anisotropic/isotropic discrepancies. It has been shown in isotropic measurements that each spectrometer and each set of acquisition parameters can lead to slight different values. This should be considered as the part of the instrumental response as any analytical methods [**60**]. However the isotopic profiles for the two types of sample are rather similar, indicating the possibility to analytically exploit isotopic data extracted from anisotropic sample.

Towards the reduction of $T_1(^{13}C)$ through the use of NMR relaxants

By accelerating the spin-relaxation mechanisms using NMR relaxants in samples, we can significantly decrease the $T_1(^{13}C)$ values, and subsequently reduce T_R and *in fine* T_{exp}. In another hand, at T_{exp} kept constant, it is also possible to add more scans for such a sample (compared to a sample without relaxant), and thus to increase the measured SNR. However, these advantages, by a significant reduction in the $T_2^*(^{13}C)$ transverse relaxation times, lead, in turn, to increase the FWHM ($\Delta\nu_{1/2}$) of ^{13}C signals, thus reducing the SNRs, and worth the spectral resolution [**64, 65, 66**]. Whatever the solvents (isotropic or anisotropic media), a balance between the gain in SNR ($T_1(^{13}C)$) and the loss of resolution ($T_2(^{13}C)$) must be find, in particular for anisotropic scalemic mixtures where the signals of two isomers are spectrally visible.

As a preliminary step, we explored the case of chromium acetylacetonate ($Cr(acac)_3$), a relaxant widely used in NMR. It has been shown that it can be used efficiently for isotropic irm-^{13}C NMR measurements [**51**]. Preliminary tests performed in liquid at 9.4 T and 315 K showed that the best compromise for **2**, between the reduction in $T_1(^{13}C)^{iso}$ and the increase in $\Delta\nu_{1/2}(^{13}C)^{iso}$ is obtained with an addition of 5 mg of relaxant for ~100 mg of solute (see **Fig. 8**) and **Tables SI-14 and 15**). Based on this result, an anisotropic sample of (*R*/*S*)-**2** was prepared with 5.0 mg

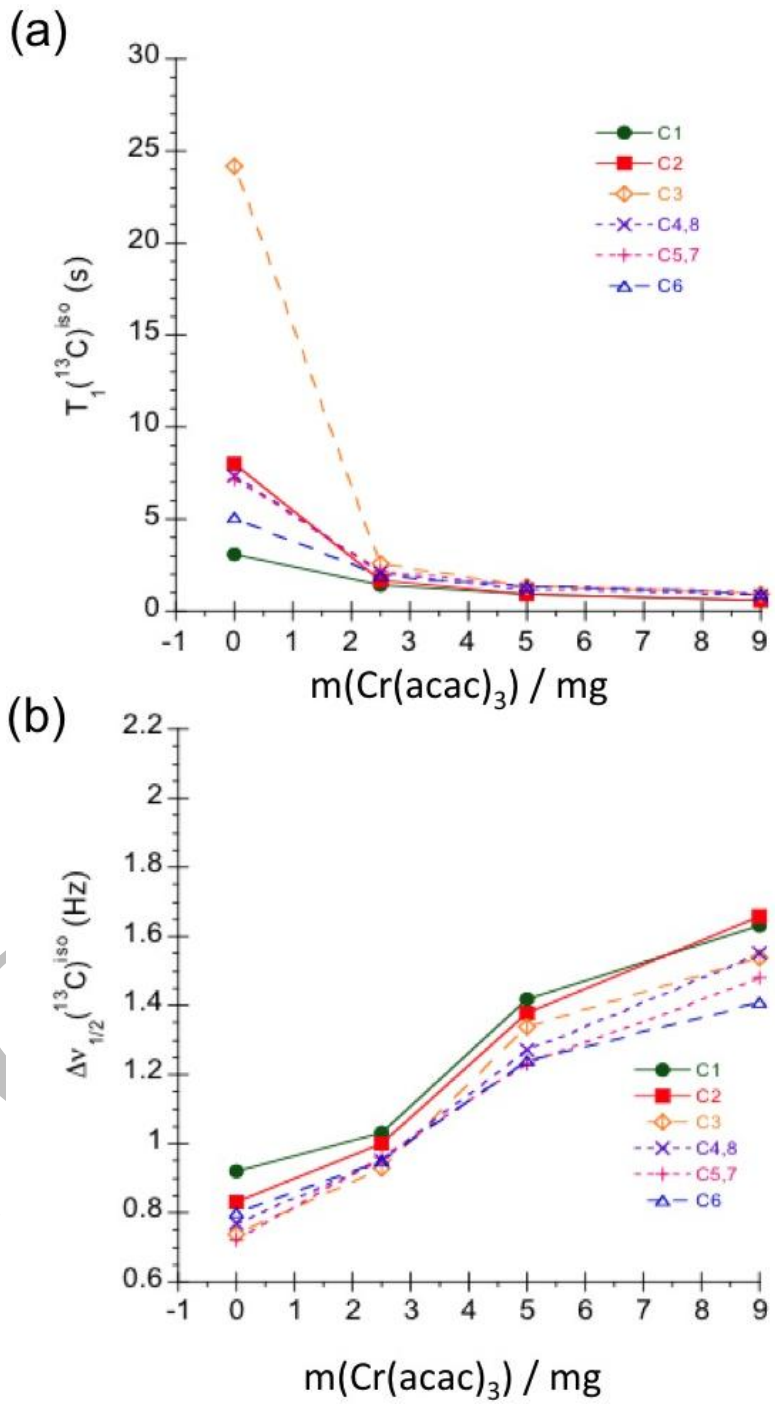

Figure 8. *Variation of (a) $T_1(^{13}C)^{iso}$ and (b) $\Delta\nu_{1/2}(^{13}C)^{iso}$ of **2** (~100 mg) in chloroform (600 mg) versus the amount of $Cr(acac)_3$ added (0.0, 2.5, 5.0 and 9.0 mg). Note the strong decrease in $T_1(^{13}C)^{iso}$ in the presence of $Cr(acac)_3$, especially for the C-3 carbon site.*

of $Cr(acac)_3$. The analysis of this anisotropic spectrum of (*R*/*S*)-**2** have pointed out again a significant decrease in $T_1(^{13}C)_i^{aniso}$ with values between 0.5 and 0.7 s, while the increase in line widths remains limited (range between 1.8 and 2.2 Hz). Such characteristics are a good compromise between a reduction in the values of $T_1(^{13}C)^{aniso}$ and a"reasonable" increase in $\Delta\nu_{1/2}$ $(^{13}C)^{aniso}$. A comparative study of the anisotropic sample of **2** with or without NMR relaxant is currently underway, but is beyond the scope of this first article.

Conclusions and perspectives

An original NMR-based quantitative spectrometric approach for potentially revealing natural $^{13}C/^{12}C$ isotopic enantiofractionations in chiral molecules is proposed. Due to the significant spectral enantiodiscriminations based on a differential enantiomeric orientation, quantitative ^{13}C-{^1H} 1D NMR in CLC's is a promising tool to access to enantiomeric isotope information, unrevealed using isotropic NMR methods (PSIA).

The main objective of this work was to examine the possibilities and the robustness of the anisotropic ^{13}C isotope quantification as well as to identify the sources of errors (sample and/or magnetic field stability, CPD scheme, …) that can affect the repeatability and reproducibility of measurements. Applied in the case of **2** oriented in PBLG-based CLC, we have demonstrated the possibility to: i) separate the enantiomeric ^{13}C signals in various carbon sites of the analyte, ii) to maximize the spectral resolutions by optimization of the sample composition, iii) to work with a very good repeatability for a series up to seven consecutive replicates; iv) to obtain a rather good long-term repeatability of results, despite the difficulties to record ^{13}C spectra (with the same sample) under strictly identical conditions due to the possible small variations of uniformity/homogeneity of the mesophase.

Clearly, these first outcomes open interesting prospects and challenging projects in the domain of the enantiomeric ^{13}C isotope fractionation analysis by anisotropic NMR. The next challenges identified will be mainly: i) the development of anisotropic ^{13}C INEPT 1D experiments to increase the sensitivity of this approach [**67, 68**], ii) the analysis of chiral AAs such as alanine which are not compatible with polypeptide-based CLCs. These challenging investigations are currently in progress.

Funding

This work was the subject of a specific grant from the CNRS as part of the ISOTOP 2018 / ISOTOP 2019 program.

Acknowledgements

The authors thank CNRS (INC) and its specific financial contribution to this project (ISOTOP 2018-2019 grant) as well as for its recurrent funding of Science. They gratefully acknowledge Mathilde Grand (CEISAM) for help with irm-MS analysis and Achille Khalid for his participation to this project in the frame of his first year of Master student's internship at ICMMO, as well as the Université Paris-Saclay (formerly, Université de Paris-Sud) for its support.

References

1. Nijenhuis I, Richnow HH, Stable isotope fractionation concepts for characterizing biotransformation of organohalides. Current Opinion in Biotechnology 2016; 41:108-113.

2. Hofstetter TB, Berg M. Assessing transformation processes of organic contaminants by compound-specific stable isotope analysis. TrAC Trends Anal.Chem. 2011;30:618-627.

3. Badea SL, Danet AF. Enantioselective stable isotope analysis (ESIA) - A new concept to evaluate the environmental fate of chiral organic contaminants. Science of the Total Environment. 2015; 514:459-466.

4. Green MM, Jain V. Homochirality in Life: Two Equal Runners, One Tripped. Orig. Life Evol. Biosph. 2010; 40:111-118.

5. Dickinson MR, Lister AM, Penkman KEH. A new method for enamel amino acid racemization dating: A closed system approach. Quaternary Geochronology. 2019;50:29-46.

6. Engel MH, Goodfriend GA, Qian Y, Macko SA. Indigeneity of organic matter in fossils: A test using stable isotope analysis of amino acid enantiomers in Quaternary mollusk shells. Proc. Nadl. Acad. Sci. USA. 1994;91:10475-10478.

7. Aelion CM, Höhener P, Hunkeler D, Aravena R, 2010. Environmental Isotopes in Biodegradation and Bioremediation. CRC; Taylor & Francis [distributor], Boca Raton, Fla; London.

8. Qiu S, Gözdereliler E, Weyrauch P, Magana Lopez EC, Kohler H-PE, Sørensen SR, Meckenstock RU, Elsner M. Small $^{13}C/^{12}C$ Fractionation Contrasts with Large Enantiomer Fractionation in Aerobic Biodegradation of Phenoxy Acids. Environ. Sci. Technol. 2014;48:5501-5511.

9. Omori AT, Gonçalves Lobo F, Gonçalves do Amaral AC, De Souza de Oliveira C. Purple carrots: Better biocatalysts for the enantioselective reduction of acetophenones than common orange carrots (*D. carota*). Journal of Molecular Catalysis B: Enzymatic. 2016;127:93–97.

10. Itoh N. Use of the anti-Prelog stereospecific alcohol dehydrogenase from Leifsonia and Pseudomonas for producing chiral alcohols. Appl Microbiol Biotechnol. 2014;98:3889-3904.

11. Corey EJ, Guzman-Perez A. The Catalytic Enantioselective Construction of Molecules with Quaternary Carbon Stereocenters. Angew. Chem. Int. Ed. 1998;37:388-401.

12. Elsila JE, Aponte JC, Blackmond DG, Burton AS, Dworkin JP, Glavin DP. Meteoritic Amino Acids: Diversity in Compositions Reflects Parent Body Histories. ACS Cent. Sci. 2016;2:370−379.

13. Neidhardt FC, Ingraham JL, Low KB, Magasanik, M. Schaechter B, Umbarger HE, Eds., Esterichia Coli and Salmonella Typhimurium. Cellular and Molecular Biology, American Society for Microbiology, 1987.

14. Ward JB. Pharmac. Ther. Biosynthesis of peptidoglycan: points of attack by wall inhibitors. 1984;25(3):327-369.

15. Amadasi A, Bertoldi M, Contestabile R, Bettati S, Cellini, B, di Salvo ML, Borri-Voltattorni C, Bossa, F, Mozzarelli A. Pyridoxal 5'-phosphate enzymes as targets for therapeutic agents. Curr. Med. Chem. 2007;14(12):1291-1324.

16. Walsh CT. Enzymes in the D-Alanine Branch of Bacterial Cell Wall Peptidoglycan Assembly. J. Biologic. Chem. 1989;264:2393-2396.

17. Fotheringham IG, Kidman GE, McArthur BS, Robinson LE, Scollar MP. Aminotransferase-Catalyzed Conversion of n-Amino Acids to L-Amino Acids. Biotechnol. Prog. 1991;7:380-381.

18. Chan-Huot M, Lesot P, Pelupessy P, Duma L, Duchambon P, Bodenhausen G, Toney MD, Reddy UV, Suryaprakash N. 'On-the-fly' kinetics of enzymatic racemization using deuterium NMR in DNA-based, oriented chiral solvents, Anal. Chem. 2013;85(9):4694-4697.

19. Finefield JM, Sherman DH, Kreitman M, Williams RM. Enantiomeric Natural products: Occurrence and Biogenesis. Angew. Chem. Int. Ed. 2012;51:4802-4836.

20. Engel K-H. Chirality: an important phenomenon regarding biosynthesis, perception, and authenticity of flavour compounds. J. Agric. Food Chem. 2020; 68:10265-10274.

21. Barabás B, Caglioti L, Micskei K, Zucchi C, Pályi G. Isotope chirality and asymmetric autocatalysis: A possible entry to biological chirality. Orig Life Evol Biosph. 2008;38:317-327.

22. Takano Y, Chikaraishi Y, Ohkouchi N. Enantiomer-specific isotope analysis (ESIA) of *D*- and *L*-alanine: nitrogen isotopic hetero- and homogeneity by microbial process and chemical process. Earth, Life, and Isotopes (edited by N. Ohkouchi, I. Tayasu, and K. Koba). Kyoto University Press., 2010, pp. 387-402.

23. Kawasaki T, Soai K. Asymmetric Induction Arising from Enantiomerically Enriched Carbon-13 Isotopomers and Highly Sensitive Chiral Discrimination by Asymmetric Autocatalysis. Bull. Chem. Soc. Jpn. 2011;84:879-892.

24. Juchelka D, Beck T, Hener U, Dettmar F, Mosandl A. Multidimensional gas chromatography coupled on-line with isotope ratio mass spectrometry (MDGC-IRMS): Progress in the Analytical. J. High Resol. Chromatogr. 1998;21:145-151.

25. Muccio Z, Jackson GP, Isotope ratio mass spectrometry, Analyst 2009;134:213-222.

26. Badea S-L, Vogt C, Gehre M, Fischer A, Danet A-F, Richnow H-H. Development of an enantiomer-specific stable carbon isotope analysis (ESIA) method for assessing the fate of □lpha-hexachlorocyclohexane in the environment. Rapid Commun. Mass Spectrom. 2011;25:1363-1372.

27. Bashir S, Fischer A, Nijenhuis I, Richnow H-H. Enantioselective carbon stable isotope fractionation of hexachlorocyclohexane during aerobic biodegradation by *Sphingobium* spp. Environ. Sci. Technol. 2013;47:11432-11439.

28. Milosevic N, Qui S, Elsner M, Einsiedl F, Maier MP, Bensch HKV, Albrechtsen H-J, Bjerg PL. Combined isotope and enantiomer analysis to assess the fate of phenoxy acids in a heterogeneous geologic setting at an old landfill. Water Res. 2013;47:637-49.

29. Maier MP, Qiu S, Elsner M. Enantioselective stable isotope analysis (ESIA) of polar herbicides. Anal. Bioanal. Chem. 2013;405:2825-2831.

30. Jammer S, Voloshenko A, Gelman F, Lev O. Chiral and isotope analyses for assessing the degradation of organic contaminants in the environment: Rayleigh dependence. Environ. Sci. Technol. 2014;48:3310-3318.

31. Jin B, Rolle M. Joint interpretation of enantiomer and stable isotope fractionation for chiral pesticides degradation. Water Res. 2016;105:178-186.

32. Liu Y, Bashir S, Stollberg R, Trabitzsch R, Weiss H, Paschke H, Nijenhuis I, Richnow H-H. Compoundspecific and enantioselective stable isotope analysis as tools to monitor transformation of hexachlorocyclohexane (HCH) in a complex aquifer system. Environ. Sci. Technol. 2017;51:8909-8916.

33. Tang B, Luo X-J, Zeng Y-H, Mai B-X. Tracing the biotransformation of PCBs and PBDEs in common Carp (*Cyprinus carpio*) using compound-specific and enantiomer-specific stable carbon isotope analysis. Environ. Sci. Technol.2017;51:2705-2713.

34. Masbou J, Meite F, Guyot B, Imfeld G. Enantiomer-specific stable carbon isotope analysis (ESIA) to evaluate degradation of chiral fungicide metalaxyl in soils. Journal of Hazardous Materials 2018;353:99-107.

35. Liu Y, Wu L, Kohli P, Kumar R, Stryhanyuk H, Nijenhuis I, Lal R, Richnow H-H. Enantiomer and carbon isotope fractionation of □-hexachlorohexane by *Sphingobium indicum* strain B90A and the corresponding enzymes. Environ. Sci. Technol. 2019;53:8715-8724.

36. Botosoa EP, Caytan E, Silvestre V, Robins RJ, Akoka S, Remaud GS. Unexpected Fractionation in Site-Specific ^{13}C Isotopic Distribution Detected by Quantitative ^{13}C NMR at Natural Abundance. J. Am. Chem. Soc. 2008;130:414-415.

37. Caytan E, Botosoa E, Silvestre, V, Robins, RJ, Akoka S, Remaud GS. Accurate quantitative C-13 NMR spectroscopy: Repeatability over time of site-specific C-13 isotope ratio determination. Anal. Chem. 2007:79(21); 8266-69.

38. Jézéquel T, Joubert V, Giraudeau P, Remaud GS, Akoka S. The new face of isotopic NMR at natural abundance, Magn. Reson. Chem. 2017;55(2)77-90.

39. Remaud GS, Giraudeau P, Lesot P, Akoka S, Isotope ratio monitoring by NMR. Part 1: Recent advances, in: G. Webb (Ed.), Modern Magnetic Resonance, Springer, Cham, 2017.

40. Robins RJ, Remaud GS, Akoka S. Isotope ratio monitoring ^{13}C nuclear magnetic resonance spectrometry for the analysis of position-specific isotope ratios, in: M.E. Harris, V.E. Anderson (Eds.), Methods in Enzymology, Vol. 596, Academic Press, Cambridge, 2017.

41. Remaud, GS, Akoka S. Isotope Ratio Monitoring by NMR. Part 3: New Applications for Traceability of Active Pharmaceutical Ingredients. In Modern Magnetic Resonance; Webb, G., Ed.; Springer, Cham, 2017.

42. Eliel EL, Wilen SH in Stereochemistry of organic compounds, John Wiley & Sons, New York, 1994.

43. Subramanian G, in Chiral separation technique, a practical approach, 2nd Ed., *Ed*. G. Subramanian, Wiley-VCH, Weimheim, 2000.

44. Wenzel TJ in Discrimination of chiral compounds using NMR spectroscopy, John Wiley & Sons, INC. New Jersey, 2007.

45. Emsley JW, Lindon JC, in NMR spectroscopy using liquid crystal solvents, Pergamon, Oxford, 1975.

46. Sarfati M, Lesot, P, Merlet D, Courtieu, J Theoretical and experimental aspects of enantiomeric differentiation using natural abundance multinuclear NMR spectroscopy in chiral polypeptide liquid crystals. Chem. Commun. 2000;2069-2081.

47. P. Lesot, C. Aroulanda, P. Berdagué, A. Meddour, D. Merlet, J. Farjon, N. Giraud, O. Lafon, Three Fertile Decades of Methodological Developments and Analytical Challenges. Prog. Nucl. Mag. Reson. Spectrosc. 2020;116:85-154.

48. Meddour A, Berdagué P, Hedli A, Courtieu J, Lesot P, Proton-decoupled carbon-13 NMR spectroscopy in a lyotropic chiral nematic solvent as an analytical tool for the measurement of the enantiomeric excess, J. Am. Chem. Soc. 1997;119(19):4502-4508.

49. Kovacs, H, Moskau D, Spraul M. Cryogenically cooled probes, a leap in NMR technology. *Prog. Nucl. Magn. Reson. Spectrosc.* 2005; 46(2-3):131-155.

50. Marathias VM, Tate PA, Papaioannou N, Massefski W. An improved method for determining enantiomeric excess by ^{13}C-NMR in chiral liquid crystal media, Chirality. 2010;22(9):838-843.

51. Caytan E, Remaud, GS. Tenailleau, E. Akoka S, Precise and accurate quantitative C-13 NMR with reduced experimental time, Talanta. 2007;71(3):1016-1021.

52. Kingsley PB, Methods of measuring spin-lattice (T_1) relaxation times: an annotated bibliography, Concepts in Magn. Reson., 1999;11(4):243-276.

53. Perch NMR Software, University of Kuopio, Finland. AC030385E.

54. Silvestre V, Mboula VM, Jouitteau C, Akoka, S, Robins RJ, Remaud GS. Isotopic ^{13}C NMR spectrometry to assess counterfeiting of active pharmaceutical ingredients: sitespecific ^{13}C content of aspirin and paracetamol, J. Pharmaceut. Biomed. Anal. 2009;50(3):336-341.

55. Craig H. Isotopic standards for carbon and oxygen and correction factors for mass-spectrometric analysis of carbon dioxide. Geochimica et Cosmochimica Acta. 1957:12(1);133-149.

56. Meija J, Coplen TB, Berglund M, Brand WA, De Bièvre P. Gröning M. Holden NE, Irrgeher J, Loss RD, Walczyk T, Prohaska T. Isotopic compositions of the elements 2013 (IUPAC Technical Report) Pure Appl. Chem. 2016;88(3):293-306.

57. Lesot P, Serhan Z, Billault I, Recent advances in the analysis of the site-specific isotopic fractionation of metabolites such as fatty acids using anisotropic natural abundance ^{2}H NMR spectroscopy: application on conjugated linolenic methyl esters. Anal. Bioanal. Chem. 2011;399(3):1187-1200.

58. Lesot P, Berdagué P, Meddour A, Kreiter A, Noll M, Reggelin M. ^{2}H and ^{13}C NMR-based enantiodetection using polyacetylene *versus* polypeptide aligning media: versatile and complementary tools for chemists. ChemPluschem. 2019;84:144-153.

59. Tenailleau E, Remaud G, Akoka S. Quantification of the ^{1}H Decoupling effects on the accuracy of ^{13}C NMR measurements, Instrum. Sci. Technol. 2005;33(4):391-399.

60. Bayle K, Gilbert A, Julien, M, Yamada K, Silvestre V, Robins RJ, Akoka S, Yoshida N, Remaud GS. Conditions to obtain precise and true measurements of the intramolecular ^{13}C distribution in organic molecules by isotopic ^{13}C nuclear magnetic resonance spectrometry. Anal. Chim. Acta 2014;846:1-7.

61. AJ, Keeler J, Freeman R. An improved sequence for broadband decoupling: WALTZ-16. J. Magn. Reson. 1983; 52: 335-338.

62. Tenaillau E, Akoka S. Adiabatic ^{1}H decoupling scheme for very accurate intensity measurements in ^{13}C NMR. J. Magn. Reson. 2007;185(1): 50-58.

63. Akoka S, Remaud GS. NMR-based isotopic and isotopomic analysis, Prog. Nucl. Magn. Reson. Spectrosc. 2020;120-121:21-24.

64. 600. Levy GC, Cargioli JD, Spin-lattice relaxation In solutions containing Cr(Iii) paramagnetic relaxation agents J. Magn. Reson. 1973; 10(2):231-234.

65. 610. Levy GC, Edlund, U. Carbon-13 chemical shift anisotropy relaxation in organic compounds. J. Am. Chem. Soc., 1975;97(17):5031-5032.

66. Differentiation of enantiomers II. In Topics in Current Chemistry, vol 341**.** Publisher: Springer International Publishing. Schurig V. editor; 2013.

67. Thibaudeau C, Remaud G, Silvestre V, Akoka S. Performance evaluation of quantitative adiabatic ^{13}C NMR pulse sequences for site-specific isotopic measurements. Anal. Chem. 2010;82:5582-5590.

68. Hajjar G, Rizk T, Bejjani J, Akoka S. Metabisotopomics of triacylglycerols from animal origin: A simultaneous metabolomic and isotopic profiling using C-13 INEPT. Food Chem. 2020;315:126325,1-8.